Journal of Optics

PAPER

A high-energy passively Q-switched Yb-doped fiber laser based on WS_2 and Bi_2Te_3 saturable absorbers

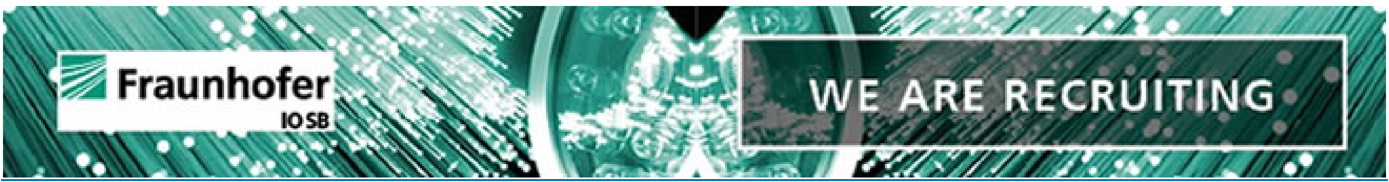

IOP Publishing Journal of Optics
J. Opt. 19 (2017) 095506 (6pp) https://doi.org/10.1088/2040-8986/aa7f5f

A high-energy passively *Q*-switched Yb-doped fiber laser based on WS_2 and Bi_2Te_3 saturable absorbers

Junli Wang[1,4], Sha Li[1], Yupeng Xing[1], Lei Chen[1], Zhiyi Wei[2] and Yonggang Wang[3]

[1] School of Physics and Optoelectronic Engineering, Xidian University, Xi'an 710071, People's Republic of China
[2] Beijing National Laboratory for Condensed Matter Physics, Institute of Physics, Chinese Academy of Sciences, Beijing 100190, People's Republic of China
[3] School of Physics and Information Technology, Shaanxi Normal University, Xi'an 710119, People's Republic of China

E-mail: dispersion@126.com

Received 14 April 2017, revised 26 June 2017
Accepted for publication 12 July 2017
Published 23 August 2017

Abstract

In this paper, we report two different saturable absorbers based on WS_2 film and Bi_2Te_3 film with similar preparation processes. A high-energy stable *Q*-switching pulse is achieved in identical cavity configurations for each absorber. A modulation depth of 10.17% and a maximum single pulse energy of 56.50 nJ are obtained when employing the WS_2 film. However, using the Bi_2Te_3 film we obtain a higher modulation depth of 23.04% and a larger single pulse energy of 61.80 nJ, and stable dual-wavelength *Q*-switching operation was shown at a pump power of 92 mW.

Keywords: WS_2, Bi_2Te_3, Q-switched laser, fiber laser

(Some figures may appear in colour only in the online journal)

1. Introduction

Passively *Q*-switched fiber lasers have many significant potential applications, for example in remote sensing, medicine, industry and fiber communications [1–3]. Methods of achieving a *Q*-switched fiber laser include active *Q*-switched operation and passive *Q*-switched operation. Compared with actively *Q*-switched fiber lasers, passively Q-switched lasers are simple, compact and flexible [4, 5]. Passive *Q*-switched operation with saturable absorbers (SAs) is widely used in pulse fiber lasers. Various types of SAs have been extensively studied and developed in the past few decades, including semiconductor saturable absorber mirrors (SESAMs) [6], single-wall carbon nanotubes (SWCNTs) [7] and graphene [8]. Graphene is the most attractive of these saturable absorbers due to its unique optoelectronic characteristics and broadband saturable absorption effect, but it lack of a bandgap limits its applications [9, 10]. In recent years, new two-dimensional (2D) nanomaterials have emerged such as topological insulators (TIs) [11], transition metal dichalcogenides (TMDs) [12, 13] and black phosphorus (BP) [14], which have attracted intense attention because of the advantages of ultra-fast recovery time and broadband saturable absorption. Compared with readily oxidizable BP, TMDs and TIs are of particular research interest.

TMDs have unique electronic and optical properties, such as indirect-to-direct bandgap transition with reducing number of layers [15]. TIs have insulating bulky states with an indirect bandgap of 0.35 eV and gapless surface states [16]. Due to their unique characteristics, they have been studied in detail. There are several examples where TMDs and TIs have been used to generate passively *Q*-switched and mode-locked fiber lasers. In 2013, Wang *et al* observed saturable absorption of MoS_2 [17]. Luo *et al* were the first to demonstrate MoS_2-based *Q*-switched fiber lasers in the wavelength range 1–2 μm [18]. Then, Lin *et al* reported a WS_2-based passively *Q*-switched fiber laser with a wide tunable range at 1.0 μm [19]. In 2012, there was the

[4] Author to whom any correspondence should be addressed.

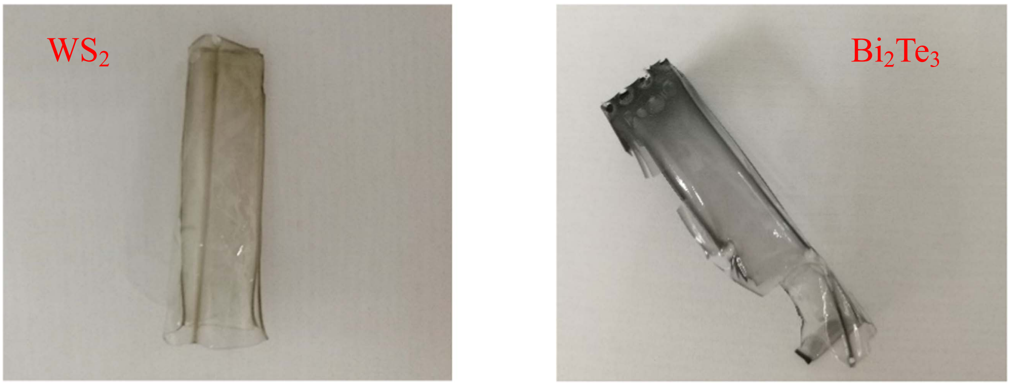

Figure 1. Photographs of WS_2 and Bi_2Te_3 films.

first demonstration of SA behavior of TIs with a Bi_2Te_3-based mode-locked fiber laser near 1550 nm [20]. Ever since that discovery, Bi_2Te_3 has been deployed in passively *Q*-switched fiber lasers with different operating wavelengths [21, 22].

In this paper, we demonstrate high-energy *Q*-switching operation based on WS_2 film and Bi_2Te_3 film in a Yb-doped ring cavity. The WS_2 and Bi_2Te_3 films are fabricated by the same simple method. A nonlinear saturable absorption experiment is carried out to measure the modulation depth of the SAs. The WS_2 film shows a modulation depth of 10.17%, and the Bi_2Te_3 film exhibits a higher modulation depth of 23.04%. We construct a high-energy Yb-doped *Q*-switched fiber laser and the results for different materials are compared based on WS_2 and Bi_2Te_3 films. Analysis of the different *Q*-switched performances provides guidance for selecting a suitable SA to satisfy the specific requirements of a *Q*-switched fiber laser.

2. Material preparation and characterization

A SA in thin-film form provides many advantages for photonic applications, such as flexibility of usage, uniform quality and mass preparation. In our experiment, WS_2–polyvinyl alcohol (PVA) and Bi_2Te_3–PVA are fabricated by a similar process. WS_2 and Bi_2Te_3 dispersions are first fabricated by a liquid-phase exfoliation method. The WS_2 and Bi_2Te_3 powders were each dispersed in deionized water, using sodium dodecyl sulfate as a surfactant. The dispersions were sonicated for 6 h, then centrifuged at 3000 rpm for 90 min. The top of the dispersions was collected by pipette. Then, the PVA power was dissolved in deionized water with ultrasonic agitation at 90 °C for 3 h. In the next step, the WS_2/Bi_2Te_3 dispersions were mixed with PVA solution and poured into polystyrene cells. Finally, these cells were put into an oven for evaporation at 40 °C. When the cells were dried, WS_2–PVA/Bi_2Te_3–PVA thin films were achieved; these can be used as SAs for *Q*-switching and mode locking. Photographs of the WS_2 and Bi_2Te_3 films are shown in figure 1.

A Raman spectroscopy system with an excitation wavelength of 633 nm was used to confirm the existence of WS_2 and Bi_2Te_3 nanosheets, as shown in figure 1. Figure 2(a) shows the in-plane vibrational mode E^1_{2g} at 350.8 cm^{-1} and the out-of-plane vibrational mode A_{1g} of WS_2 at 420.2 cm^{-1}. Three typical Raman optical photon peaks of Bi_2Te_3 are shown in figure 2(b), which are identified as ${A_{1g}}^1$ at 61 cm^{-1}, ${E_g}^2$ at 101 cm^{-1} and ${A_{1g}}^2$ at 133 cm^{-1}.

Nonlinear saturable absorption is the key parameter for evaluating a SA. We built a twin-detector measurement system to investigate the saturable absorption of WS_2–PVA and Bi_2Te_3–PVA thin films. In the system, a stable home-made picosecond pulsed laser source (central wavelength 1029.8 nm, pulse duration 4.1 ps, repetition rate 27.22 MHz) worked as the illuminator. The measurement results are shown in figure 3. The fitting formula is [23]

$$T(I) = 1 - \Delta T \times \exp(-I/I_{\text{sat}}) - A_{\text{ns}}$$

where T is transmittance, ΔT is modulation depth, I is intensity of laser, I_{sat} is saturation power intensity and A_{ns} is non-saturable absorbance. Figure 3(a) shows that the modulation depth (MD) of the WS_2-PVA thin film is 10.17%, the saturating intensity about 8.89 MW cm^{-2} and the non-saturable loss about 3.41%. As can be seen from figure 3(b), the Bi_2Te_3-PVA thin film exhibits a MD of 23.04%, which is higher than that of the WS_2-PVA thin film, a saturating intensity of 22.55 MW cm^{-2} and a non-saturable loss of 48.39%.

3. Experiment setup

Figure 4 shows the experimental setup for the passively *Q*-switched Yb-fiber laser based on WS_2–PVA thin film. The ring laser oscillator cavity comprises a wavelength division multiplexer (WDM), a gain fiber, a polarization-independent isolator (PI-ISO), a polarization controller (PC), a WS_2–PVA thin film and an optical coupler (OC). A 30 cm long Yb-doped fiber (Liekki Yb 1200-4/125) with an absorption coefficient of 1200 dB m^{-1} at 976 nm was used as the gain medium. The 60% port of an optical coupler is used for the laser output. The fiber laser is core pumped with a laser diode emitting at 975.4 nm, with a maximum output power of 700 mW. The PI-ISO was used to force unidirectional operation in the fiber ring cavity. The PC was employed in the cavity to optimize *Q*-switched operation. The SA film was cut

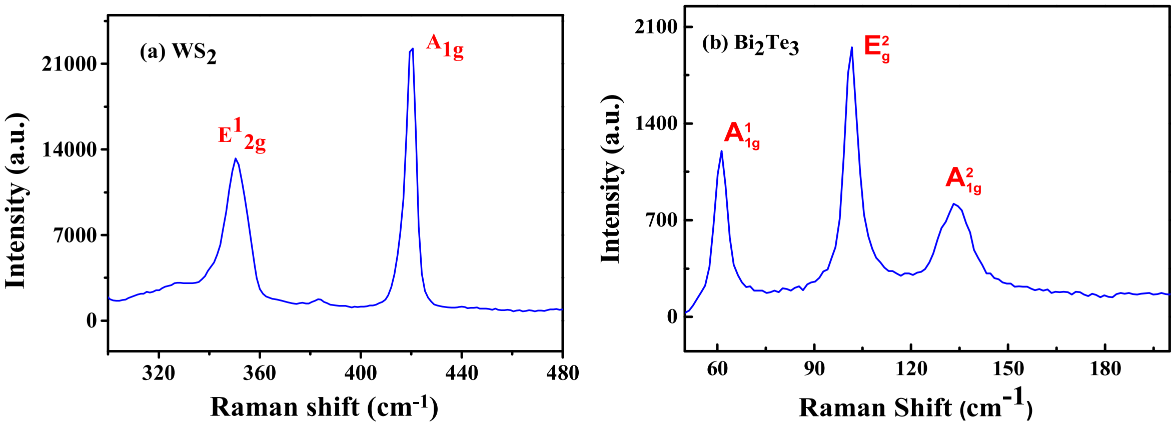

Figure 2. Raman spectra of (a) WS_2 and (b) Bi_2Te_3.

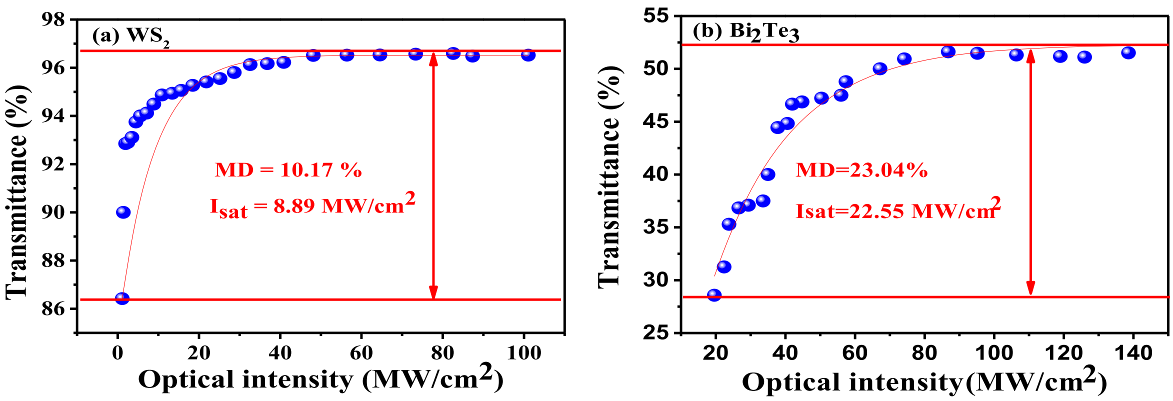

Figure 3. (a) Nonlinear absorption of the WS_2–PVA SA. (b) Nonlinear absorption of the Bi_2Te_3–PVA SA.

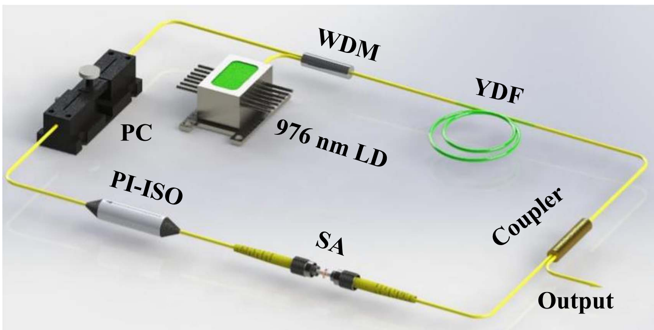

Figure 4. Diagram of the experimental setup.

into a small film of 1 mm × 1 mm. The small SA film was transferred onto the standard FC/APC fiber end face. The fiber core was entirely covered by the film. The standard FC/APC fiber with the SA film was connected with the other clean one by a standard flange adapter, forming an all-fiber structure. The architecture of the passively Q-switched Yb-fiber laser based on the Bi_2Te_3–PVA thin film was completely the same; only the SA needs to be changed.

4. Results and discussion

Q-switching operation is obtained based on the two types of SA as follows. When the pump power is increased gradually, free running of the continuous wave (CW) laser is first observed. When the pump power is further increased, Q-switched pulses are generated at a certain pump power for different SA materials. The WS_2 Q-switching operation starts at a pump power of 50 mW, and Bi_2Te_3 starts when the pump power is higher than 60 mW. Figure 5 shows the stable Q-switching pulse trains of WS_2 and Bi_2Te_3 at a certain pump power. Figure 5(a) shows that the repetition rate of the Q-switching pulse based on WS_2 is 53.80 kHz at a pump power of 72 mW, corresponding to a pulse interval of 18.58 μs. Figure 5(b) shows that the repetition rate of the Q-switching pulse based on Bi_2Te_3 is 75.39 kHz at a pump power of 88 mW, corresponding to a pulse interval of 13.26 μs. A larger scanning range of the pulse-train under 100 μs is also presented in the insets of figures 5(a) and (b).

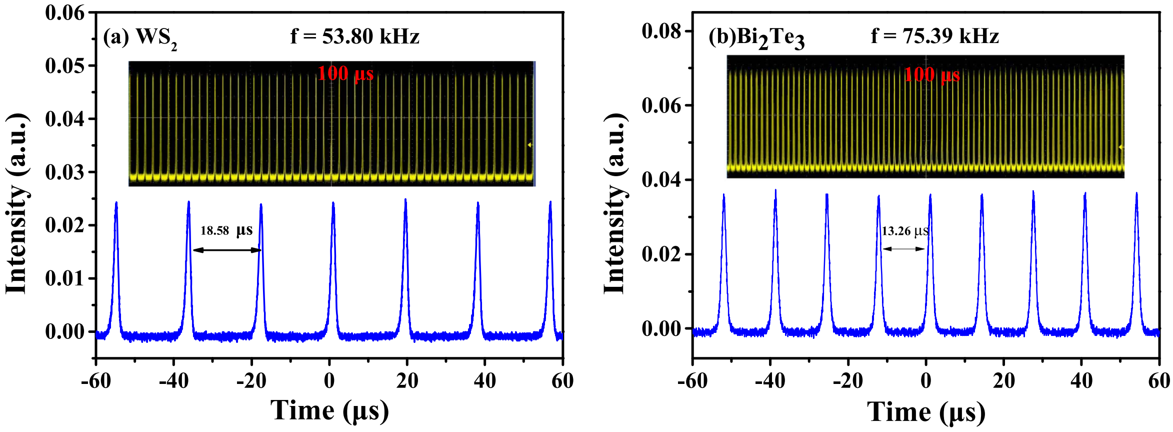

Figure 5. Stable Q-switching pulse trains of WS_2 and Bi_2Te_3 at a certain pump power.

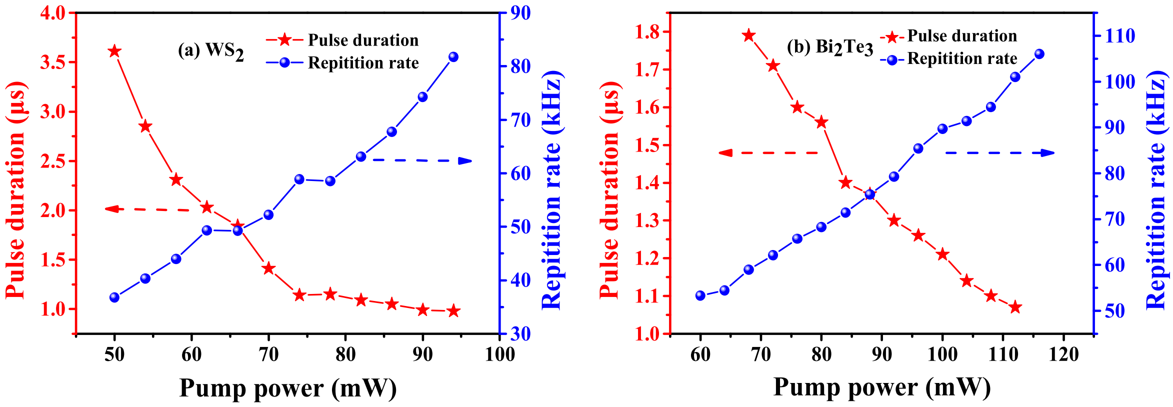

Figure 6. Pulse duration and repetition rate versus incident pump power.

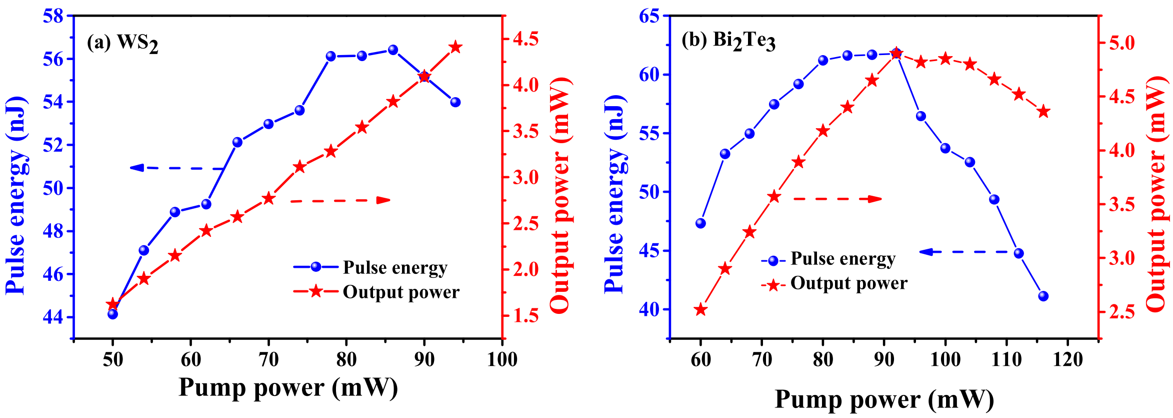

Figure 7. Output power and single pulse energy versus incident pump power.

Figure 6 shows the evolution of the repetition rate and pulse duration with pump power; these are typical features of Q-switching operation. Figure 6(a) shows that the repetition rate of WS_2 pulse trains increases linearly from 36.78 kHz to 81.75 kHz with the increase in pump power, corresponding to the pulse duration reducing from 3.61 μs to 1.0 μs. Figure 6(b) shows that the repetition rate of Bi_2Te_3 pulse trains increases linearly from 53.31 kHz to 106 kHz, while the pulse duration varies in the range 1.79 μs to 1.07 μs. It can be concluded that Bi_2Te_3 has higher the repetition rate than WS_2 under the maximum pump power, which is an obvious advantage. The shortest pulse duration of the two is very similar. The pulse duration can be further narrowed by shortening the ring laser cavity and increasing the modulation depth of the SA [24–26].

The output power and single pulse energy can be varied by increasing the pump power. This relationship is described in figure 7. The maximum single pulse energy based on WS_2 and Bi_2Te_3 are 56.50 nJ and 61.80 nJ, respectively, under the

Table 1. Typical Q-switched results based on WS_2 and Bi_2Te_3 in the 1.0 μm band in recent reports.

SA	Repetition rate (kHz)	Pulse duration (μs)	Maximum pulse energy (nJ)	Modulation depth (%)	Reference
WS_2	24.9–36.7	3.2	13.6	3.1	[27]
WS_2	60.2–97.0	1.65	28.8	3.87	[19]
WS_2	36.78–81.75	3.61–1.0	56.50	10.17	Our work
Bi_2Te_3	35–77	1.0–1.3	38.3	2.5	[21]
Bi_2Te_3	53.31–106.0	1.79–1.07	61.80	23.04	Our work

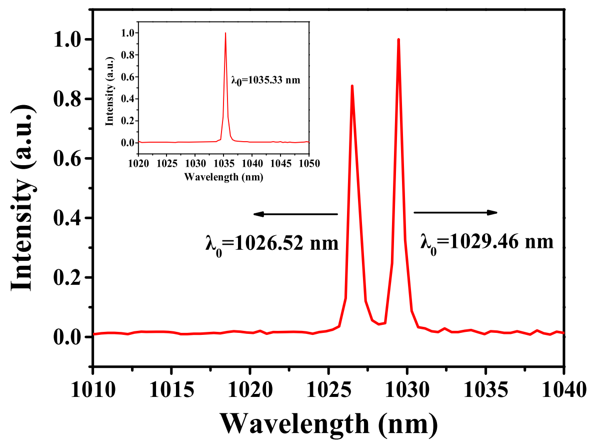

Figure 8. The dual-wavelength lasing spectrum of the Q-switched Yb-doped fiber laser based on Bi_2Te_3 at a pump power of 92 mW. Inset: CW laser output spectrum with a Bi_2Te_3 SA in the cavity.

same pump power. From figure 7(b), we observe that the output power and single pulse energy are reduced under a high incident pump power, but stable Q-switching still occurs. It may be that Bi_2Te_3 suffers from two-photon absorption under a high incident pump power. In figure 7, when the pump power exceeded 94 mW and 116 mW, for WS_2 and Bi_2Te_3, respectively, the Q-switching state becomes unstable. If the pump power is increased further, the Q-switching state disappears. A stable Q-switching state can be obtained again by decreasing the pump power. The unstable Q-switching phenomenon may be attributed to oversaturation rather than to thermal damage, as typically observed in some other passively Q-switched fiber lasers [23–25]. In table 1, we compare the results for passively Q-switched fiber lasers at the 1.0 μm wave band based on WS_2 and Bi_2Te_3 SAs. Compared with other reports, it is noted that the maximum single pulse energy and the shortest pulse duration of Bi_2Te_3 and WS_2 are achieved in our work, which is mainly due to the high modulation depth of the SAs.

Finally, when we carefully adjust the PC, stable dual-wavelength Q-switching operation with Bi_2Te_3 was achieved under a pump power of 92 mW (as observed by the optical spectrum analyzer). As shown in the figure 8, there was dual-wavelength simultaneous oscillation at 1026.52 nm and 1029.46 nm. The dual-wavelength output possess a wavelength spacing of 2.94 nm. In order to confirm the dual-wavelength output resulting from the Bi_2Te_3, we also measured the CW spectrum without the Bi_2Te_3, which is shown in the inset of figure 8. The center wavelength of the CW spectrum is 1035.33 nm. Because such a dual-wavelength fiber laser has potential applications in microfiber photonics research, microwave carriers and high bit-rate pulses it has gained wide attention [28].

5. Conclusion

In summary, a high-energy Q-switched Yb-doped fiber laser based on WS_2 and Bi_2Te_3 SAs has been demonstrated. WS_2 shows a modulation depth of 10.17% while Bi_2Te_3 exhibits a modulation depth of 23.04%. The maximum single pulse energy based on these SAs are 56.50 nJ and 61.80 nJ, respectively. Stable dual-wavelength Q-switching operation was achieved with Bi_2Te_3. Comparing the two kinds of SA, Bi_2Te_3 has obvious advantages.

References

[1] Adachi S and Koyamada Y 2002 Analysis and design of Q-switched erbium-doped fiber lasers and their application to OTDR *J. Lightwave Technol.* **20** 1506–11

[2] Paschotta R, Haring R, Gini E, Melchior H, Keller U, Offerhaus H L and Richardson D J 1999 Passively Q-switched 0.1 mJ fiber laser system at 1.53 μm *Opt. Lett.* **24** 388–90

[3] Skorczakowski M *et al* 2010 Mid-infrared Q-switched Er: YAG laser for medical applications *Laser Phys. Lett.* **7** 498–504

[4] Wang Y, Chen H, Shen D, Zhang J and Tang D 2013 High power continuous-wave and graphene Q-switched operation of Er: YAG ceramic lasers at ~1.6 μm *J. Opt. Soc. Korea* **17** 5–9

[5] Luo Z, Zhou M, Weng J, Huang G, Xu H, Ye C and Cai Z 2010 Graphene-based passively Q-switched dual-wavelength erbium-doped fiber laser *Opt. Lett.* **35** 3709–11

[6] Yang W, Hou J, Zhang B, Song R and Liu Z 2012 Semiconductor saturable absorber mirror passively Q-switched fiber laser near 2 μm *Appl. Opt.* **51** 5664–7

[7] Im J H, Choi S Y, Rotermund F and Yeom D I 2010 All-fiber Er-doped dissipative soliton laser based on evanescent field interaction with carbon nanotube saturable absorber *Opt. Express* **18** 22141–6

[8] Choi S Y, Jeong H, Hong B H, Rotermund F and Yeom D 2014 All-fiber dissipative soliton laser with 10.2 nJ pulse energy using an evanescent field interaction with graphene saturable absorber *Laser Phys. Lett.* **11** 015101

[9] Liu J, Wu S, Yang Q and Wang P 2011 Stable nanosecond pulse generation from a graphene-based passively Q-switched Yb-doped fiber laser *Opt. Lett.* **36** 4008–10

[10] Wang Q H, Kalantar-Zadeh K, Kis A, Coleman J N and Strano M S 2012 Electronics and optoelectronics of

two-dimensional transition metal dichalcogenides *Nat. Nanotechnol.* **7** 699–712
[11] Zhao C, Zhang H, Qi X, Chen Y, Wang Z, Wen S and Tang D 2012 Ultra-short pulse generation by a topological insulator based saturable absorber *Appl. Phys. Lett.* **101** 211106
[12] Huang Y, Luo Z, Li Y, Zhong M, Xu B, Che K, Xu H, Cai Z, Peng J and Weng J 2014 Widely-tunable passively Q-switched erbium-doped fiber laser with few-layer MoS_2 saturable absorber *Opt. Express* **22** 25258–66
[13] Zheng X, Zhang Y, Chen R, Cheng X, Xu Z and Jiang T 2015 Z-san measurement of the nonlinear refractive index of monolayer WS_2 *Opt. Express* **23** 15616–23
[14] Sotor J, Sobon G, Macherzynski W, Paletko P and Abramski K M 2015 Black phosphorus saturable absorber for ultrashort pulse generation *Appl. Phys. Lett.* **107** 051108
[15] Radisavljevic B, Radenovic A, Brivio J, Giacometti V and Kis A 2011 Single-layer MoS_2 transistors *Nature Nanotechnol* **6** 147–50
[16] Chen Y L *et al* 2009 Experimental realization of a three-dimensional topological insulator, Bi_2Te_3 *Science* **325** 178–81
[17] Wang K, Wang J, Fan J, Lotya M, Neill A O, Fox D, Feng Y, Zhang X, Jiang B and Zhao Q 2013 Ultrafast saturable absorption of two-dimensional MoS_2 nanosheets *ACS Nano* **7** 9260–7
[18] Luo Z, Huang Y, Zhong M, Li Y, Wu J, Xu B, Xu H, Cai Z, Peng J and Weng J 2014 1-, 1.5-, and 2-μm fiber lasers Q-switched by a broadband few-layer MoS_2 saturable absorber *J. Lightwave Technol.* **32** 4077–84
[19] Lin J, Hu Y, Chen C, Gu C and Xu L 2015 Wavelength-tunable Yb-doped passively Q-switching fiber laser based on WS_2 saturable absorber *Opt. Express* **23** 29059–64
[20] Bernard F, Zhang H, Gorza S P and Emplit P 2012 Towards mode-locked fiber laser using topological insulators in nonlinear photonics *Nonlinear Photonics NP 2012 (Colorado Springs, CO, 17–21 June 2012)* (Optical Society of America)
[21] Lee J, Koo J, Chi C and Lee J H 2014 All-fiberized, passively Q-switched 1.06 μm laser using a bulk-structured Bi_2Te_3 topological insulator *J. Opt.* **16** 085203
[22] Lee J *et al* 2015 Passively Q-switched 1.89 μm fiber laser using a bulk-structured Bi_2Te_3 topological insulator *IEEE J. Sel. Top. Quant.* **21** 0900206
[23] Chen Y *et al* 2015 Mechanically exfoliated black phosphorus as a new saturable absorber for both Q-switching and mode-locking laser operation *Opt. Express* **23** 12824–33
[24] Yu Z, Song Y, Tian J, Dou Z, Guoyu H, Li K, Li H and Zhang X 2014 High-repetition-rate Q-switched fiber laser with high quality topological insulator Bi_2Se_3 film *Opt. Express* **22** 11508–15
[25] Li H, Xia H, Lan C, Li C, Zhang X, Li J and Liu Y 2015 Passively Q-switched erbium-doped fiber laser based on few-layer MoS_2 saturable absorber *IEEE Photon. Technol. Lett.* **27** 69–71
[26] Luo Z, Huang Y, Weng J, Cheng H, Lin Z, Xu B, Cai Z and Xu H 2013 1.06 μm Q-switched ytterbium-doped fiber laser using few-layer topological insulator Bi_2Se_3 as a saturable absorber *Opt. Express* **21** 29516–22
[27] Zhang M, Hu G, Hu G, Howe R C T, Chen L, Zheng Z and Hasanl T 2015 Yb- and Er-doped fiber laser Q-switched with an optically uniform, broadband WS_2 saturable absorber *Sci. Rep.* **5** 17482
[28] Rahman M T, Rashid F A, Ahmad H, Azzuhri S R, Razak M Z A and Faruki M J 2017 Dual-wavelength ytterbium-doped fiber laser using microfiber and D-shaped polished fiber *Optik* **130** 1421–5